Journal of Energy and Natural Resources
2022; 11(2): 44-51
http://www.sciencepublishinggroup.com/j/jenr
doi: 10.11648/j.jenr.20221102.13
ISSN: 2330-7366 (Print); ISSN: 2330-7404 (Online)

Geochronology and Geochemistry of Felsite Dike from Shanmen Silver Deposit in Central Jilin Province, China, and Its Geological Significance

Cremilda Samuel Jofrisse*, Pei Yao, Chai Sheli*

College of Geo-Exploration Science and Technology, Jilin University, Changchun, China

Email address:

cremildajofrisse@hotmail.com (C. S. Jofrisse), peiyao@jlu.edu.cn (Pei Yao), chaisl@jlu.edu.cn (Chai Sheli)

*Corresponding author

To cite this article:

Cremilda Samuel Jofrisse, Pei Yao, Chai Sheli. Geochronology and Geochemistry of Felsite Dike from Shanmen Silver Deposit in Central Jilin Province, China, and Its Geological Significance. *Journal of Energy and Natural Resources*. Vol. 11, No. 2, 2022, pp. 44-51.
doi: 10.11648/j.jenr.20221102.13

Received: May 9, 2022; **Accepted**: June 6, 2022; **Published**: June 8, 2022

Abstract: Shanmen silver deposit is located on the south section of Daheishan horst polymetallic mineralization belts in central Jilin province, Northeast China. The deposit supplies not only the greatest portion of silver in Jilin province, and a significant amount of gold also. The deposit exhibits a closely spatiotemporal relationship with Mesozoic ore-hosting diorite and granite intrusions and Mesozoic basic-felsic dikes. Among the dikes the felsite one occurred at the same fault zone as the silver-bearing veins in the deposit, implying that felsite dike has an important theoretical and ore-prospecting significance. Here, we mainly investigate felsite dike based on zircon LA-ICP-MS U-Pb geochronology, petrochemical compositions. Zircon U-Pb dating from felsite dike yielded a weighted mean age of 163.1± 2.3 Ma, which is slightly younger than the ore-hosted intrusions of quartz diorite (167.6± 1.9 Ma) and monzonite granite (167.0 ± 1.5 Ma), indicating that petrogenetic age of felsite dike is late Jurassic. Major element data suggest that felsite dike is of granodioritic and granitic in chemical composition, belonging to high-K calc-alkaline and shoshonite series, with SiO_2, K_2O+Na_2O, Al_2O_3, TiO_2, CaO and MgO contents ranging from 62.98-79.18%, 4.13-5.3%, 13.31-16.01%, 0.05-0.57%, 0.15-3.07%, and 0.28-1.8%, respectively. Felsite dike is enriched in Rb, U, and Pb, and depleted in Ba, Nb, Sr, Ti and other high field strength elements. REE contents of felsite dike are in the range of 28.42-214.23 ppm, showing weak negative Eu anomalies with Eu/Eu* ratios of 0.24-0.61. Except for the altered felsite sample with SiO_2 content of 79.18%, the distribution characteristics of trace elements and rare earth elements in felsite dike are similar with those of ore-hosted intrusion of granite and diorite. The geochemical features show that late Jurassic felsite dike was formed in the tectonic background of active continental margins associated with subduction in the Paleo-Pacific Plate. The underplating of mantle-derived magma caused the partial melting of the meta-sediment in lower crust materials to form the mid-late Jurassic magmatism and late Jurassic silver mineralization.

Keywords: Zircon U-Pb Geochronology, Major and Trace Elements, Felsite Dike, Shanmen Silver Deposit

1. Introduction

Shanmen silver deposit is a large-scale deposit only discovered in Jilin Province, Northeast China, which is located on the south section of Daheishan horst in Xing'an-Mongolian Orogenic Belt [1]. The deposit supplies not only the greatest portion of silver production in Jilin province, and a significant amount of gold resource also. The deposit has a closely spatiotemporal relationship with Mesozoic ore-hosted diorite and granite intrusions and Mesozoic basic-felsic dikes. Among dikes the felsite one, so called as the dike of coeval metallogenetic epoch, was commonly occupied the same fault zones as the silver-bearing quartz veins in the deposit, implying that to investigate felsite dike is the important ways to understand the ore genesis and to summarize the ore prospecting indicators. The deposit was first explored in 1982. Since that time a lot of studies about the geological characteristics and the metallogeny of the silver deposit, the petrology, geochronology, and geochemistry of ore-hosting intrusions [2-10], etc., were carried out. However,

only a few studies were involved in the petrological characteristics, geochronology of various dikes occurred in the deposit [3, 4]. Geologically, unravelling the magmatic and metallogenic events in one given area is mostly reliable on precise radioactive dating of the objective geological bodies. Previous researchers in the study area provided some radioactive dating results of ore-hosting intrusions, dikes, and silver ores, however, the dating methods they used were dominated by K-Ar dating of K-bearing mineral separates and whole-rock samples [5], U-Th-Pb dating of zircon mineral separates [5], and Rb-Sr dating of fluid inclusions trapped in quartz from silver ores [10]. Therefore, it is hard to provide the accurate and reliable ages constraint for silver mineralization and Mesozoic magmatic events because of poorly representatives of dated samples and larger analytical errors caused by those dating methods. The accurate forming age of dikes closely related to the silver mineralization is still unknown, and the relationship between the ore-hosted intrusions and various dikes exposed in the silver mine area is poorly understood. LA-ICP-MS was applied to U–Pb zircon dating in the 1990s [11], which has since become the most rapidly used method of U-Pb dating method owing to its high spatial resolution, rapid analysis time, and affordability relative to secondary ion mass spectrometry [11].

In order to summarize the metallogeny and origin of gold and silver deposits in the mid-east part of Jilin province, a program, research on the metallogeny of the typical ore deposits in Jilin province, funded by Geological Fund of Jilin province, was carried out between 2019 and 2021, in which the geochemical characteristics and ore-forming ages of Shanmen silver deposit were investigated. This study is contributed from above program. The main objectives of this study are to present the latest LA-ICP-MS zircon U-Pb dating data and major and trace element content data of felsite dike closely associated to silver mineralization in Shanmen silver deposit, then to constraint the metallogenic ages of silver mineralization U-Pb dating, and finally to deduce the source rock and petrogenetic settings of felsite dike with those data.

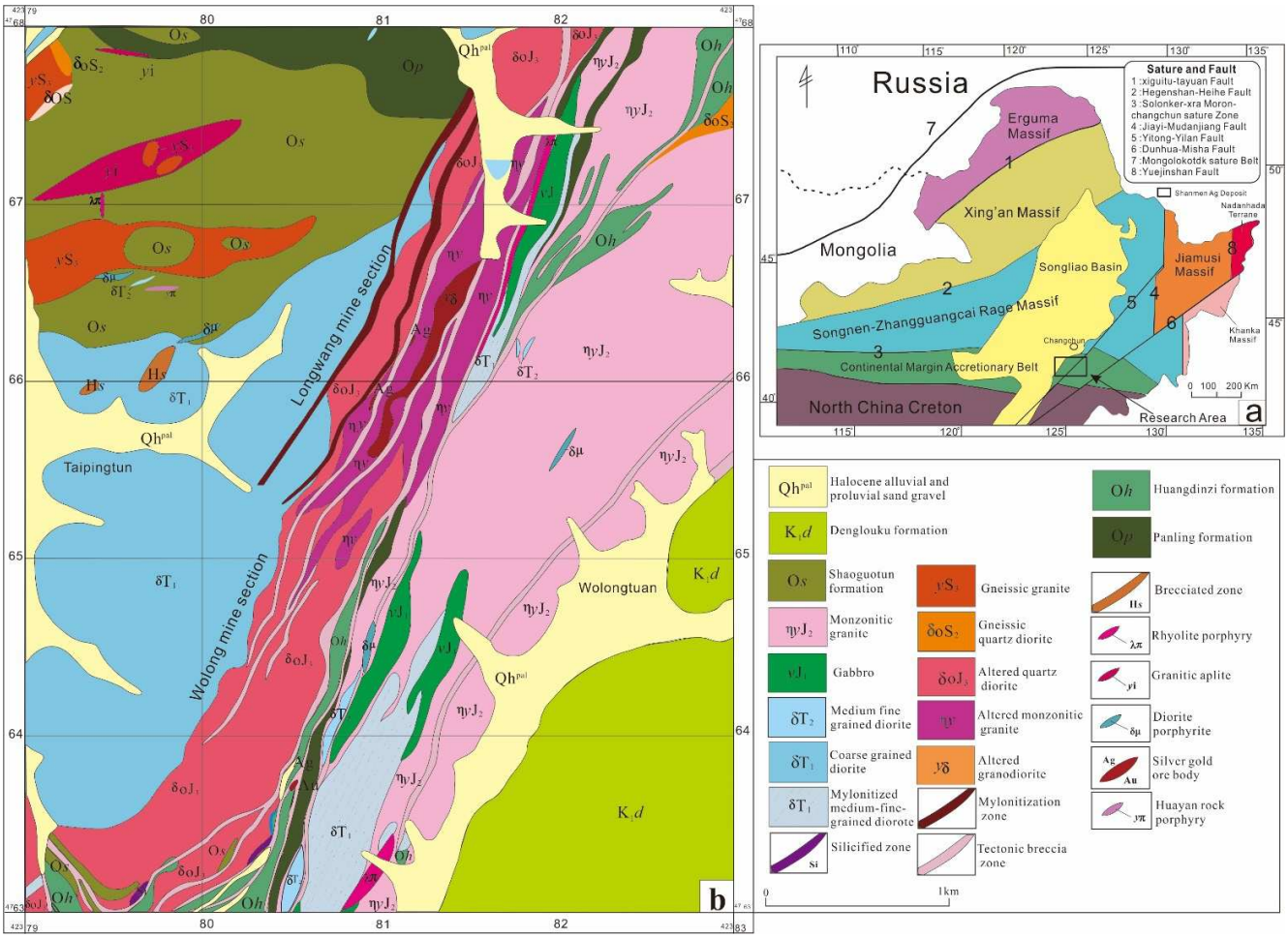

Figure 1. *(a) Tectonic sketch map of Northeast China, modified after Zhang [4]; (b) Geological map of Shanmen silver mine in Siping city, Jilin province.*

2. Geological Settings

The studied area is situated at the southeast Siping city, central Jilin Province, Northeast China. The tectonic setting of the area is located on Daheishan horst within Xing'an -Mongolian Orogenic Belt [1], and in the continental margins accretionary belt (Figure 1a). The strata exposed in the study area are of Paleozoic, Mesozoic and Quaternary. Paleozoic strata are the Ordovician Panling Formation (meta-rhyolite, meta-dacite with

meta-siltstone), the Huangdingzi Formation (banded marble, nodule marble with metasiltstone), the Shaoguotun Formation (meta-argillaceous fine-grained sandstone, feldspar granulite, biotite plagioclase granulite). Mesozoic strata are the Denglouku Formation (feldspathic quartz arenite, siltstone with thin layer mudstone). Quaternary is mainly composed of Holocene alluvial and diluvial sediments. Silver ore bodies in Wolong mine section in Shanmen silver deposit are hosted in the Huangdingzi Formation.

The intrusive rocks in the study area can be grouped into three episodes: (1) the mid-late Silurian gneissic granite and gneissic quartz diorite of the early Paleozoic, only occurred in Shaoguotun Formation as small stocks; (2) the mid-early Triassic medium-fine-grained and coarse-grained diorites of the Mesozoic; (3) the mid-late Jurassic intrusions of altered quartz diorite (LA-ICP-MS, 167.6 ± 1.9 Ma) [8, 9] and monzonite granite (LA-ICP-MS, 167.0 ± 1.5 Ma) [8, 9], and the various Jurassic dikes. Both intrusions exposed as larger stocks, and monzonite granite is the host rock of Ag-bearing quartz veins in Longwang mine section in the silver deposit. The dikes can be divided into three stages according to their temporal relationships with the silver mineralization: the early stage of dikes prior to the silver ores, such as fine monzonite granite; the coeval stage of dikes with the silver ores, such as felsite dike, which intruded the early the altered and silicified country rocks (Figure 2a, b), and then cross-cut by the fine silicified quartz veins (Figure 2c, d) of the main silver mineralization period; the later stage of dikes after the silver ores, including lamprophyre (whole-rock K-Ar, 122 Ma) [5], diabase porphyry, diorite porphyry (LA-ICP-MS, 160.1 ± 2.2 Ma) [8, 9], granite porphyry, rhyolite porphyry (whole-rock K-Ar, 67 Ma) [5], and granite aplite.

The studied area is predominately controlled by NE-striking faults, among them Yitong-Yilan deep fault (Figure 1a) and its derived ones are the major ore- and intrusive rock-controlling structures. The Shanmen silver deposit can mainly be divided into two mining sections (Figure 1b): Wolong mine section in the south of the deposit, in which the ore host rocks are chiefly the marble in Huangdingzi Formation, and mineralized type belongs to the altered ore; Longwang mine section in the north of the deposit, in which the ore host rocks are mainly the mid-late Jurassic altered quartz diorite and monzonite granite, and mineralized type is the Ag-bearing quartz veins. Shanmen silver deposit is a hydrothermal vein-type deposit closely associated with Mesozoic intrusions and dikes [8].

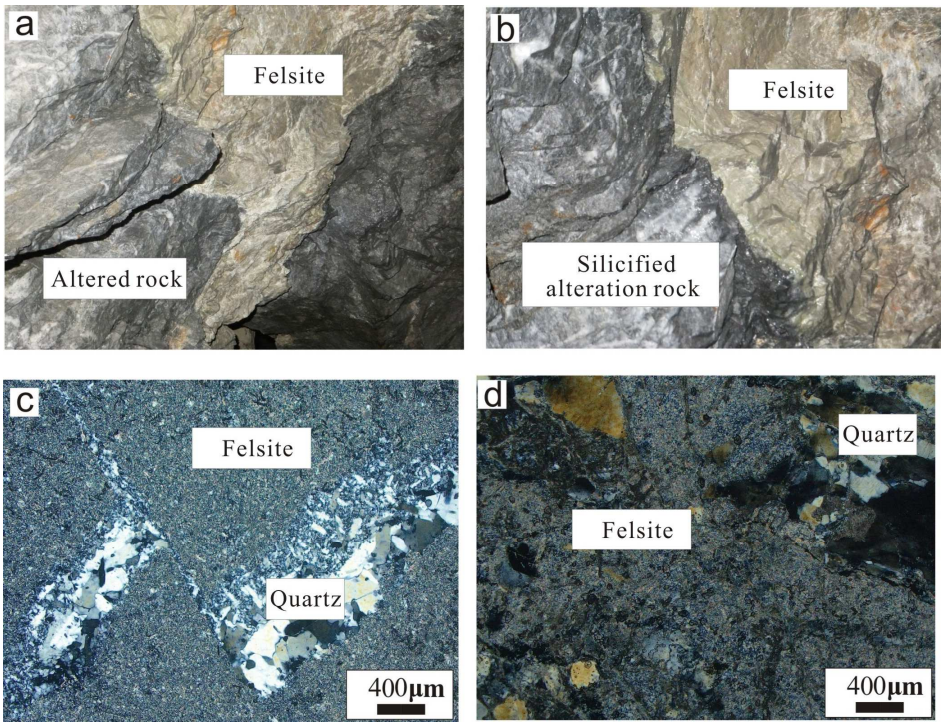

Figure 2. *Field photos (a, b) and micrographs (c, d) of felsite dike in Shanmen silver deposit.*

3. Analytical Methods

The felsite dike samples for Zircon U-Pb dating and element content analyses were collected from the working adit of the sixth mining level in Wolong mine section. Felsite dike displays the felsic texture, a variant of microcrystalline texture, comprised by microcrystal grains of plagioclase, potassium feldspar and quartz. The felsite dike apparently underwent the strong silicification and sericite alteration. The zircons in felsite dike sample were separated at the Langfang Regional Geological Survey in Hebei Province, China. The handpicked zircons were photographed under reflected and transmitted light, and zircon zonation structures were observed by zircon grain imaging of cathodoluminescence (CL). Zircon U-Pb dating was carried out using LA-ICP-MS at the Key Laboratory of Mineral Resources Evaluation in Northeast Asia, Ministry of Land and Resources, Jilin

University, China. All the analytical procedures where used description as Yuan et al [12]. A laser beam spot with a diameter of 32μm and a frequency of 7 Hz was used for sample analysis; isotope ratios, age values and errors were calculated with GLITTER software [13]; common lead correction was carried out on the results using Andersen's method [14]; age harmony and graph plotting were calculated with Isoplot program [15]. Major, trace element and rare earth element contents of bulk-rock samples of felsite dike were measured at ALS Minerals-ALS Chemex (Guangzhou, China) Co., Ltd. The major element contents of the felsite dike samples were determined using lithium metaborate and lithium tetraborate fusion by X-ray fluorescence (XRF). The contents of trace elements in the felsite dike samples were measured using four-acid digestion (HCl, HNO_3, HF, and $HClO_4$) by ICP-MS. The contents of rare earth elements were analyzed using lithium tetraborate fusion by ICP-MS.

4. Results and Discussion

4.1. Zircon U-Pb Ages

The Cathodoluminescence (CL) images of zircons from felsite dike are seen in Figure 3, and U-Pb concordia age and average age histograms of zircons from felsite dike are represented in Figure 4. Most zircons in the felsite dike are short-long columnar, euhedral-subhedral, having 50-100μm in size and 1:1-2:1 as aspect ratio. Zircon grains mostly show magmatic oscillatory or planar zoning, and some zircons show core-rim textures (Figure 3). A total of 20 spots were analyzed on 20 zircon grains from one felsite sample (Table 1). The concentrations of U and Th in zircons are 87.41-2736.1 ppm and 93.58-1033.35 ppm (Table 1), respectively. Th/U values in zircons range from 0.14 to 1.47, with an average value of 0.54, implying their magmatic origin. $^{206}Pb/^{238}U$ ages of 20 analyzed zircon grains are in the range of 159-169 Ma. These zircons yield a weighted average age of 163.1 ± 2.3 Ma with an MSWD of 0.31 (Figure 4), indicating that the petrogenetic age of felsite dike is late Jurassic, which is slightly younger than the ore-hosted intrusions, and slightly older than the dike of diorite porphyry.

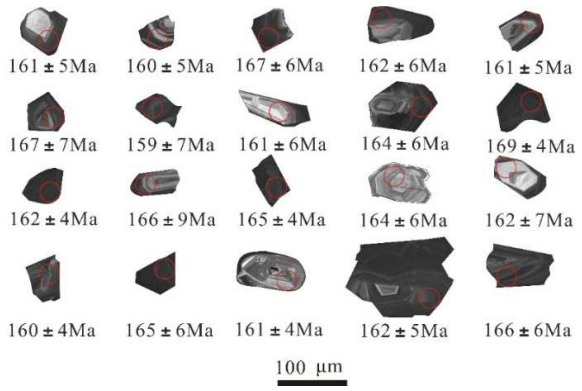

Figure 3. *Cathodoluminescence (CL) images of zircons from felsite dike.*

4.2. Geochemistry

4.2.1. Major Elements

The felsite dike is characterized by medium-high silica contents (62.98%–79.18%), and extremely low contents of Na_2O (0.01-0.01%), MnO (0.05-0.08%), TiO_2 (0.05-0.57%), and P_2O_5 (0.07-0.15%). In the plot of K_2O+ Na_2O with SiO_2 (Figure 5a), felsite dike falls into the field of granodiorite and granite, diorite porphyry into that of monzonite and monzonite gabbro, quartz porphyry and granite porphyry into that of granite, fine-grained monzonite into that of quartz monzonite, diabase porphyry into that of monzonite gabbro, lamprophyre into that of monzonite gabbro and foid-gabbro, diorite into that of monzonite, monzonite gabbro, monzonite diorite, diorite, and foid- gabbro, and granite that of into granite and quartz monzonite. It can be concluded that the Mesozoic intrusive rocks and dikes are of the basic-acidic, and only the mid-late Jurassic intermediate-acid rocks are closely associated with the formation of silver deposit. In plot of K_2O with SiO_2 (Figure 5b), the felsite dike belongs to the high-K calc-alkaline and shoshonite series, diorite porphyry to the shoshonite and calc-alkaline series, quartz porphyry, granite porphyry and fine-grained monzonite to the high-K calc–alkaline series, diabase porphyry and lamprophyre to the shoshonite series, diorite intrusion mostly to the high-K calc-alkaline series, with less the shoshonite and calc–alkaline series, granite intrusion mostly to the high-K calc-alkaline.

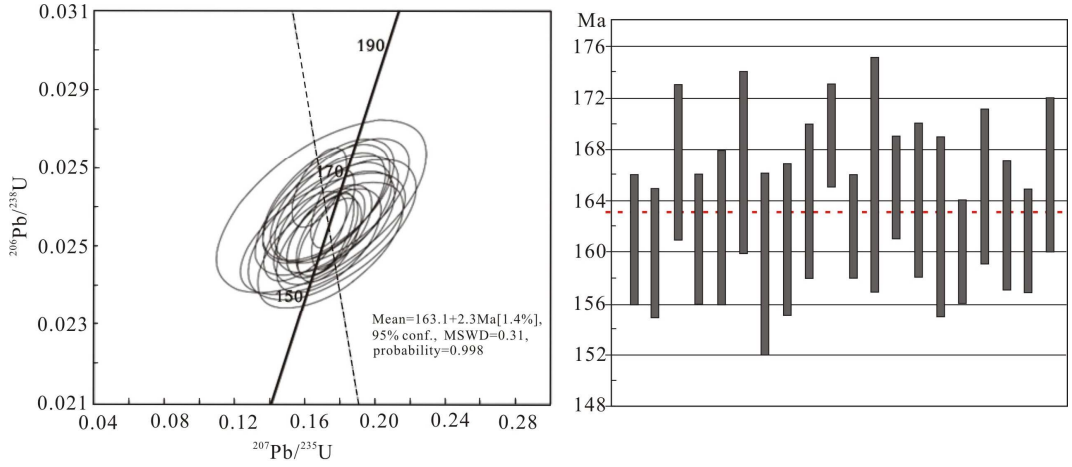

Figure 4. *U-Pb concordia diagram and mean age histograms of zircons from felsite dike.*

Table 1. *Results of zircon LA-ICP-MS U-Pb dating of felsite dike in Shanmen silver deposit.*

Spot	Pb (10^{-6})	Th (10^{-6})	U (10^{-6})	Th/U	$^{207}Pb/^{206}Pb$	$^{207}Pb/^{235}U$	$^{206}Pb/^{238}U$	$^{207}Pb/^{206}Pb$	1σ	$^{207}Pb/^{235}U$	1σ	$^{206}Pb/^{238}U$	1σ
A04	33.04	93.58	314.98	0.30	0.04921	0.17186	0.02533	158	136	161	13	161	5
A07	134.94	789.21	1228.19	0.64	0.05012	0.17368	0.02513	201	190	163	17	160	5
A08	46.79	155.55	427.64	0.36	0.04802	0.17334	0.02619	100	232	162	21	167	6
A10	60.25	222.77	497.98	0.45	0.04605	0.16038	0.02526	155	208	151	14	161	5
A11	108.24	347.12	996.16	0.35	0.05042	0.17696	0.02546	214	219	165	20	162	6
A12	110.8	432.02	975.2	0.44	0.04989	0.17999	0.02617	190	246	168	22	167	7
A17	80.96	617.71	722.9	0.85	0.05062	0.1747	0.02503	224	265	163	24	159	7
A18	10.638	128.22	87.41	1.47	0.04877	0.17022	0.02532	137	295	160	27	161	6
A20	118.59	305.07	1091.33	0.28	0.04978	0.17657	0.02573	185	206	165	19	164	6
A21	340.3	395.3	2736.1	0.14	0.04605	0.16823	0.0265	91	145	158	9	169	4
A24	179.15	428.58	1676.75	0.26	0.05025	0.17592	0.02539	207	59	165	7	162	4
A25	103.34	716.66	856.97	0.83	0.04729	0.16956	0.02601	64	325	159	34	166	9
A26	101.74	382.71	911.86	0.42	0.04912	0.17571	0.02595	154	63	164	7	165	4
A30	15.58	149.11	128.43	1.16	0.04851	0.17255	0.0258	124	254	162	23	164	6
A32	103.43	1033.35	852.38	1.22	0.0501	0.17553	0.02542	200	287	164	27	162	7
A33	237.03	961.44	2172.7	0.44	0.05022	0.17419	0.02516	205	107	163	10	160	4
A37	63.75	237.14	559.77	0.42	0.04864	0.17434	0.026	131	201	163	18	165	6
A38	211.03	468.35	1961.13	0.24	0.04968	0.17385	0.02538	180	147	163	14	162	5
A39	80.74	235.42	741.59	0.32	0.04956	0.17267	0.02528	174	104	162	10	161	4
A40	157.84	345.68	1424.65	0.24	0.04784	0.17207	0.02609	91	230	161	21	166	6

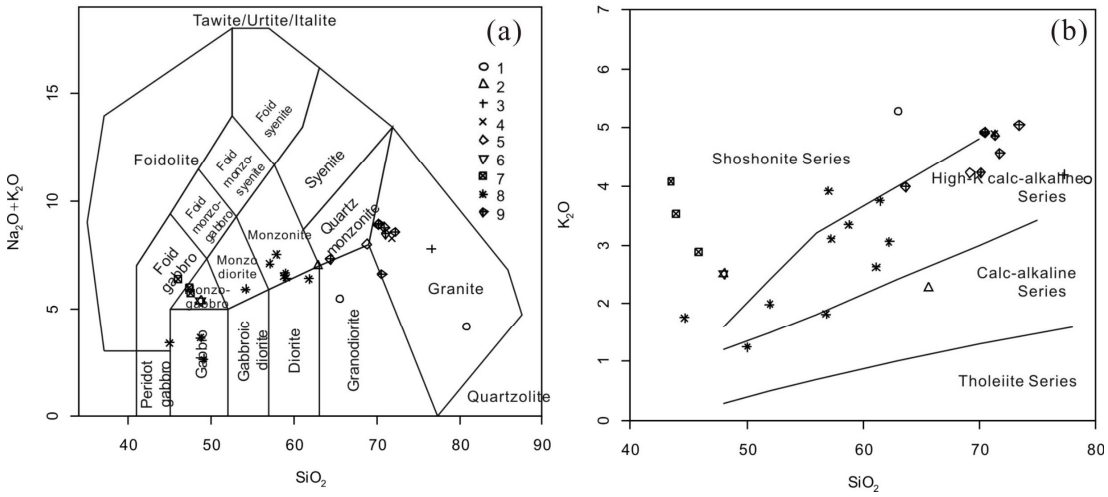

Figure 5. *(a) Total alkali (Na_2O+K_2O) against SiO_2 (after Middlemost, 1994) [16]; (b) K_2O against SiO_2 plot (after Peccerillo and Taylor, 1976) [17]. 1-felsite; 2-diorite porphyry; 3-quartz porphyry; 4-granite porphyry; 5-fine-grained monzonite; 6-diabase porphyry; 7-lamprophyre; 8-quratz diorite; 9-monozonite granite.*

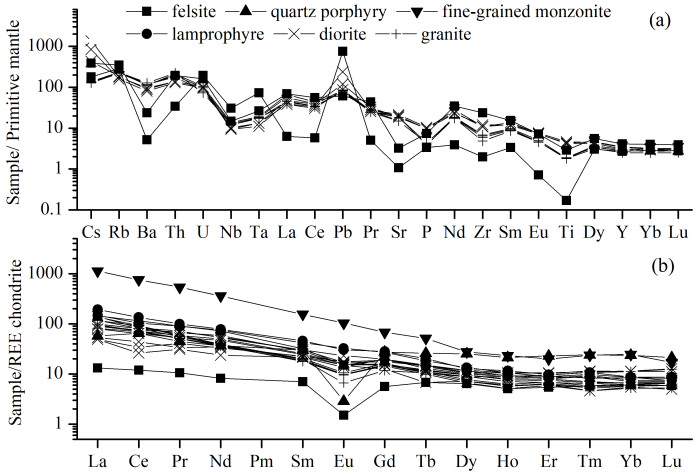

Figure 6. *(a) Spider diagram of trace element (primitive mantle values from Sun and McDonough, 1995) [18]; (b) Chondrite-normalized REE patterns (chondrite REE values from Boynton, 1984) [19].*

4.2.2. Trace Elements

Felsite is enriched in Rb, U, Pb, depleted in Ba, Nb, Sr, Ti and other high field strength elements (Figure 6a). REE contents of felsite dike are in the range of 28.42-214.23 ppm, showing weak negative Eu anomalies with Eu/Eu* ratios of 0.24-0.61. Except for the altered felsite sample with SiO_2 content of 79.18%, the distribution characteristics of trace elements (Figure 6a) and rare earth elements (Figure 6b) in felsite dike are similar with those of ore-hosted intrusion of granite and diorite, implying that intrusions and dikes including felsite are derived from the same sources.

4.3. Metallogenic Age of Silver Deposit

Geologically, the metallogenic age of Shanmen silver deposit should be later than the forming ages of ore-hosted altered quartz diorite (167.6 ± 1.9 Ma) [8, 9] and monzonite granite (167.0 ± 1.5 Ma) [8, 9], but earlier than of diorite porphyry (160.1± 2.2 Ma) [8, 9] after the silver ores. Felsite dike not only intruded the early silicified alteration rocks, and cross-cut by the white silicified veins of the main silver mineralization period also, implying that felsite dike is coincident to silver mineralization. Felsite dike is dated at 163.1 ± 2.3 Ma by method of zircon U-Pb dating in the study, indicating that the accurate metallogenic age of silver deposit is approximately 163 Ma ranging from about 160 Ma to 168 Ma. Therefore, in view of silver ore prospecting the felsite dike with low contents of Na_2O, MnO, TiO_2 and P_2O_5 and the dated age of around 163 Ma is a good indicator for silver exploration during the regionally geological survey.

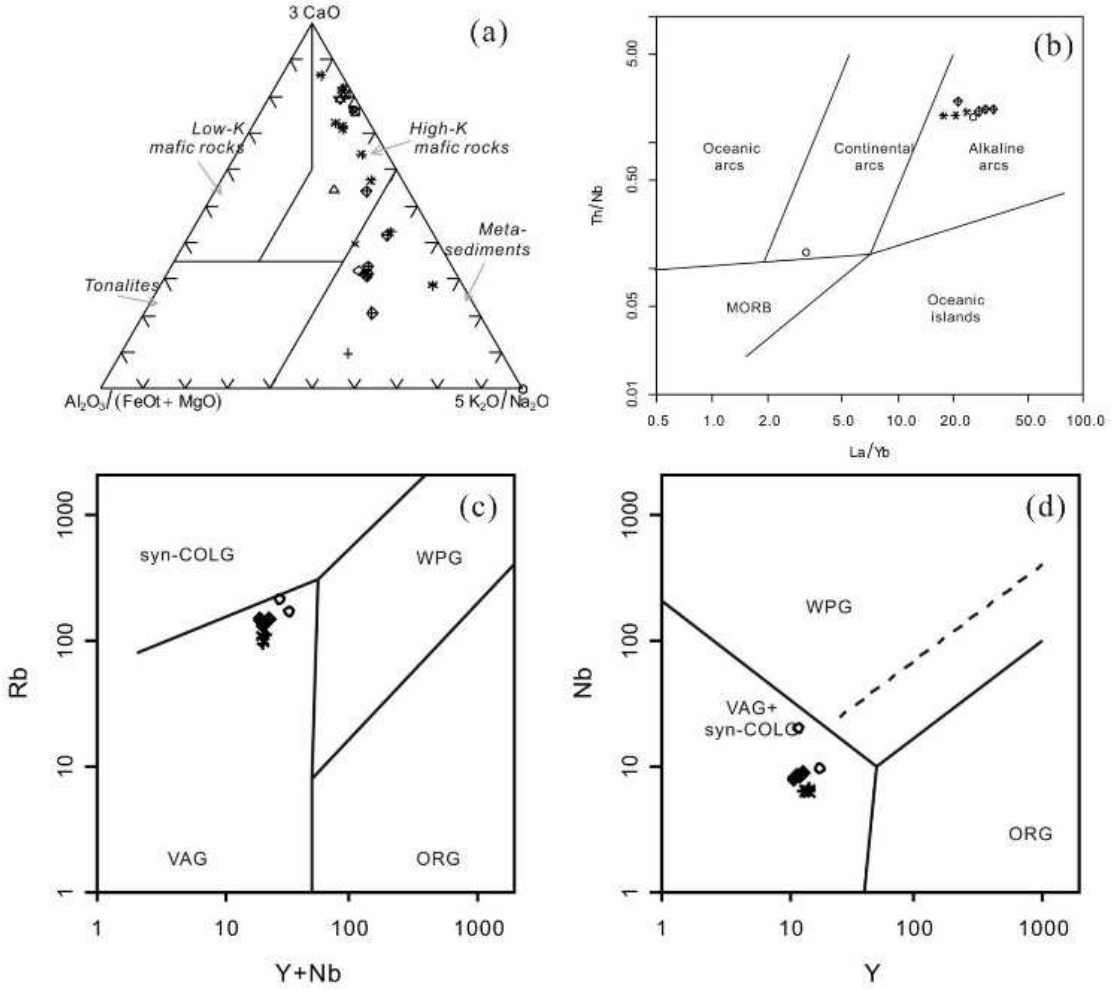

Figure 7. *(a) $Al_2O_3/(FeO+MgO)–5K_2O/Na_2O-3CaO$ (after Laurent et al, 2014) [20]; (b) Th/Nb-La/Yb plot (after Hollocher et al, 2012) [21]; (c) Y+Nb with Rb plot (after Pearce et al, 1984) [22]; (d) Y against Nb plot (after Pearce et al, 1984) [22].*

4.4. The Source Rock and Petrogenetic Settings of Felsite

It can be seen form Figure 7a that the rock source of mid-late Jurassic intrusions and dikes those which are closely related with the silver mineralization were mainly derived from high mafic rocks and meta-sediments. Felsite has extremely low contents of Na_2O, so the plotted point location in Figure 7a is far away from other dikes or intrusive rocks. Dikes of felsite, quartz porphyry, granite porphyry, and fine-grained monzonite with high silica contents, and ore-hosted intrusion of monzonite granite were mainly derived from the source of meta-sediments in lower crust,

while dikes of diabase porphyry, lamprophyre with low level of silica, and ore-hosted intrusion of quartz diorite were mainly contributed from the source of high mafic rocks.

In Figure 7b, ore-hosted intrusions of quartz diorite and monzonite granite are plotted in alkaline arcs, and felsite dike falls into alkaline arcs except for the altered one. The ore-hosted intrusions of quartz diorite and monzonite granite, and felsite dike were plotted in volcanic arc granite and syn-collision granite (Figure 7c, d). It can be deduced from this study that late Jurassic felsite dike, together with mid-Jurassic ore-hosted intrusions of quartz diorite and monzonite granite, was formed in the tectonic background of active continental margins associated with subduction in the Paleo-Pacific Plate. The fluid released by the dehydration of the subduction slab during subduction continuously replaced the mantle wedges, which induced the partial melting of mantle wedges, leading to forming a mantle-source basalt magma. The underplating of mantle-derived basalt magma caused the partial melting of the meta-sediment in lower crust materials to form basic-acidic magma enriched silver and gold. Finally, the mid-late Mesozoic ore-hosted intrusions and dikes were formed through differentiation and crystallization of the magma.

5. Conclusion

Felsite dike in Shanmen silver deposit is closely related with the silver mineralization in the time and space, therefore, it can be used as a direct indicator for silver exploration in the studied area and its adjacent area.

The age of felsite dike dated by zircon U-Pb in Shanmen silver deposit is 163.1 ± 2.3 Ma, implying that metallogenic age of silver mineralization in the studied area is of late Jurassic.

Felsite dike is characterized by extremely low Na_2O content, which belongs to high-K calc–alkaline and shoshonite series. The magmas from which the mid-late Jurassic ore-hosted intrusions and dikes crystallized were derived through partial melting of lower continental crust with some input of mantle materials, those which were formed in the active continental margins associated with subduction in the Paleo-Pacific Plate.

Acknowledgements

This study was supported by the geological funds of Jilin province (Grants 2018DK36-24). We would like to thank Zi Xuejun, the chief manager in Shanmen silver deposit, who gave some useful help during the field geological survey and sampling samples of rock and ores in the underground of the Shanmen silver deposit. We would also like to thank Li Wenqing, the senior engineer in the Key Laboratory of Mineral Resources Evaluation in Northeast Asia, Ministry of Land and Resources, Jilin University, China, who provided a useful contribution to the research works during the zircon U-Pb testing.

References

[1] S. Zhigang, H. Zuozhen, G. Lihua, G. Hongyan, L. Xuping, M. Fanxue, H. Mei, A. Wenjian, L. Jingjing, D. Qingxiang, Y. Junlei, and L. Hui, "Permo-Triassic evolution of the southern margin of the Central Asian Orogenic Belt revisited: Insights from late Permian igneous suite in the Daheishan horst, NE China," Gondwana Res., 2018, vol. 56, pp. 23-50.

[2] T. Weisheng, S. Jianbo, "Geological characteristis of the Shanmen silver deposit in Siping, Jilin Provice, "Miner. Depos., 1991, vol. 10, pp. 152-160 (Chinese with English abstract).

[3] W. Fukuan, "Genesis of the Mesozoic intrusive rock in the Shanmen silver mining and the relation to the metallogeny," Jilin Geol., 1992, pp. 20-33 (Chinese with English abstract).

[4] Z. Ming, "Geologic characteristics and metallogenic prognosis in deep and periphery in Shanmen silver deposit of Siping city, Jilin province," Master thesis of Jilin University, 2005. unpublised.

[5] H. Wenbin, S Haoche,"Isotopic geochemistry evidence for genesis of shanmen silver deposit, Siping,"Geology and Prospecting, 2006, vol. 40, pp. 46-60 (Chinese with English abstract).

[6] F. Ming, C. Li, Z. Pengfu, and C. Lixin, "Geological characteristics and prospecting indicators of Shanmen silver deposit in Siping, Jilin province," Geol. Resour., 2010, vol. 13, pp. 215-220 (Chinese with English abstract).

[7] W. Zhigang, "Study on metallogenesis of Mesozoic endogenetic metal deposits in the eastern part of Jilin province," Doctoral dissertation of Jilin University, 2012. unpublished.

[8] S Xinhao, R. Yunshen. C. Peng, H. Yujie, and G. Yu, "Ore genesis of Shanmen Ag deposit in Siping area of southern Jilin province, NE China: Constraints from fluid inclusions and H-O, S, Pb isotopes, "Minerals, 2019, pp. 1-29.

[9] C. Peng, "Ore genesis and tectonic setting of Shanmen Ag deposit in Siping area, Jilin province," Master thesis of Jilin University, 2020. unpublised.

[10] L. Huaying, W. Xiuzhang, C. Jingping, "Rb-Sr isotope age and the time scale of hyhdrothermal activities for the Siping Ag(Au) deposit, Jilin province," Geotecton. Metallog., 2001, vol. 25, pp. 194-198 (Chinese with English abstract).

[11] B. Schoene, "U-Th-Pb geochronology," in Treatise on Geochemistry, H. D. Holland, K. K. Turekian, Eds., 2nd, Elsevier, Oxford, 2014, pp. 341-378.

[12] H. Yuan, S. Gao, X. Liu, H. Li, D. Günther, and F. Wu, "Accurate U-Pb age and trace element determinations of zircon by laser ablation-inductively coupled plasma-mass spectrometry, Geostand,"Geoanalytical Res., 2004, vol. 28, pp. 353-370.

[13] W. Griffin, W. Powell, N. J. Pearson, and S. O'Reilly," GLITTER: data reduction software for laser ablation ICP-MS," Short Course Ser., 2008, vol. 40, pp. 308-311.

[14] T. Andersen, "Correction of common lead in U-Pb analyses that do not report 204Pb," Chem. Geol., 2002, vol. 192, pp. 59-79.

[15] K. R. Ludwig, "User's manual for a geochronological toolkit for Microsoft Excel (Isoplot/Ex version 3.0)," Spec. Publ., 2003, No 4. 4, pp. 1-71.

[16] E. A. Middlemost, "Naming materials in the magma/igneous rock system," Earth-Science Reviews, 1994, vol. 37, pp. 215-224.

[17] A. Peccerillo, S. R. Taylor S R, "Geochemistry of Eocene calc-alkaline volcanic rocks from the Kastamonu area, Northern Turkey," Contrib Mineral Petrol., 1976, vol. 58, pp. 63-81.

[18] W. F. McDonough, and S. S. Sun, "The composition of the Earth," Chemical Geology, 1995, vol. 120, pp. 223-253.

[19] W. V. Boynton, "Cosmochemistry of the rare earth elements; meteorite studies," In Rare Earth Element Geochemistry, P. Henderson, Ed., Elsevier, Amsterdam, 1984, pp. 63-114.

[20] O. Laurent, H. Martina, J. F. Moyena, R. Doucelance,"The diversity and evolution of late-Archean granitoids: evidence for the onset of "modern-style" plate tectonics between 3.0 and 2.5 Ga," Lithos, 2014, vol. 205, pp. 208-235.

[21] K. Hollocher, P. Robinson, E. Walsh, and D. Roberts," Geochemistry of amphibolite-facies volcanics and gabbros of the Støren Nappe in extensions west and southwest of Trondheim, Western Gneiss Region, Norway: a key to correlations and paleotectonic settings, "American Journal of Science, 2012, Vol. 312, pp. 357-416.

[22] J. A. Pearce, N. W. Harris, and A. G. Tindle, "Trace element discrimination diagrams for the tectonic interpretation of granitic rocks," J. Petrol, 1984, vol. 25, pp. 956-983.